Localized detection of action potential-induced presynaptic calcium transients at a *Xenopus* neuromuscular junction

David A. DiGregorio and Julio L. Vergara *

Department of Physiology, UCLA School of Medicine, Los Angeles, CA 90095, USA

1. Action potential (AP)-induced fluorescence transients were measured, using Ca^{2+} indicators and a spot-detection method, at single nerve terminals of a cultured *Xenopus* neuromuscular junction preparation with simultaneous measurement of neurotransmitter release.

2. Transients obtained using the low affinity Ca^{2+} indicator Oregon Green™ 488 BAPTA-5N (OGB-5N) exhibited rapid rising ($t_{½}$ (time at which one-half of the peak fluorescence was attained) = 0·54 ms) and decaying (τ_{fast} = 1·9 ms) phases. The higher affinity indicator Oregon Green™ 488 BAPTA-2 (OGB-2) produced transients with significantly slower kinetics ($t_{½}$ = 2 ms; τ_{slow} = 73 ms).

3. Tetanic stimulation elicited distinct increases in fluorescence in response to each AP. Each OGB-5N fluorescence increase was more rapid than those observed using OGB-2. Furthermore, a smaller proportion of residual fluorescence at the end of the train was observed using OGB-5N.

4. When OGB-5N was used, a significant [Ca^{2+}] increase was observed prior to the release of neurotransmitter. This was not observed when OGB-2 was used.

5. We conclude that the use of localized optical detection coupled with low affinity Ca^{2+} indicators can help elucidate rapid changes in presynaptic [Ca^{2+}] dynamics underlying evoked neurotransmitter release.

In 'fast' synapses, the action potential (AP)-induced release of neurotransmitter occurs within a millisecond and depends on the entry of Ca^{2+} into the nerve terminal (Katz, 1969). According to the modern view of the Ca^{2+} hypothesis of neurotransmission (Augustine, Charlton & Smith, 1987), an AP invades the nerve terminal and opens voltage-sensitive Ca^{2+} channels, thereby rapidly increasing the local [Ca^{2+}] to 100–500 μM at discrete submembrane regions or microdomains (Llinás, Sugimori & Silver, 1995). A Ca^{2+} sensor then initiates the fusion of neurotransmitter-containing synaptic vesicles (Augustine *et al.* 1987).

Much of what has been inferred about the kinetics and magnitude of the highly localized [Ca^{2+}] changes in synaptic terminals is derived from mathematical models (Simon & Llinás, 1985; Zucker & Fogelson, 1986). However, experimental measurement of these [Ca^{2+}] changes has been hampered by their high degree of localization and by kinetic limitations imposed by [Ca^{2+}] detection methodologies. The advent of 'fast' Ca^{2+} indicators (molecular probes that rapidly equilibrate with Ca^{2+} (in ~1 ms)) has made the assay of ensemble presynaptic AP-induced Ca^{2+} transients in multicellular preparations and the investigation of their relationship to neurotransmitter release possible (Sabatini & Regehr, 1996; Sinha, Wu & Saggau, 1997). Moreover, these studies highlighted the kinetic differences between transients measured using fast (low affinity) and slow (high affinity) indicators. Previous work in the squid giant synapse, using aequorin and arsenazo III as Ca^{2+} indicators (Llinás & Nicholson, 1975; Miledi & Parker, 1981; Charlton, Smith & Zucker, 1982), demonstrated that intracellular [Ca^{2+}] changes in response to single APs could be measured in a single cell simultaneously with a postsynaptic response. However, the slow response and complex stoichiometry of these Ca^{2+} indicators compromised the ability to establish a cause and effect relationship between single Ca^{2+} transients and neurotransmitter release.

In the present study, we have employed patch-clamp and spot-detection (Escobar, Monck, Fernandez & Vergara, 1994) methods in a cultured *Xenopus* neuromuscular junction preparation (Yazejian, DiGregorio, Vergara, Poage, Meriney & Grinnell, 1997). Using fluorescent Ca^{2+} indicators, we recorded AP-induced transients at single nerve terminals with submillisecond temporal resolution and submicron spatial resolution. The experimental results

* To whom correspondence should be addressed.

This manuscript was accepted as a Short Paper for rapid publication.

allow us to infer kinetic properties of $[Ca^{2+}]$ changes at presynaptic microdomains underlying neurotransmitter release at a 'fast' synapse.

METHODS

Solutions

Neuronal patch electrodes were backfilled with an internal solution of the following composition (mM): 90 potassium aspartate, 20 KCl, 30 Mops, 2 $MgCl_2$, 0·2 EGTA, 2 ATP-Mg, 0·5 GTP-Na_2, and 2 phosphocreatine, pH 7·0 (6–10 MΩ resistance). Either 300 μM Oregon Green™ 488 BAPTA-5N (OGB-5N) or 50 μM Oregon Green™ 488 BAPTA-2 (OGB-2) (Molecular Probes, Eugene, OR, USA) was added. The dye-containing solution was treated with Calcium Sponge™ S (Molecular Probes) to remove contaminating free Ca^{2+}, and filtered with a 0·2 μm nylon filter (Nalgene, Rochester, NY, USA). The myocyte patch electrode internal solution contained (mM): 80 caesium aspartate, 15 CsCl, 15 Mops, 2 $MgCl_2$, 10 EGTA (to minimize myocyte contractility), 2 ATP-Tris, 0·5 GTP, and 2 phosphocreatine, pH 7·0 (2–3 MΩ resistance).

Normal frog Ringer solution (NFR), consisting of (mM): 114 NaCl, 2·5 KCl, 10 Mops, 1·8 $CaCl_2$, and 10 dextrose (pH 7·0), was used to bathe the cultures during recording periods. In experiments in which we did not patch clamp the myocyte (8 out of 26), 10 μM curare was added to NFR to block synaptically evoked myocyte contraction.

Cell culture imaging and fluorescence spot detection

Nerve–muscle co-cultures were prepared from dissociated neural chord tissue obtained from embryos as described previously (Yazejian *et al.* 1997). In brief, stage 20–22 *Xenopus laevis* embryos were rinsed in sterile 10% NFR and then killed by severing the neural tube region. Isolated neural and somite tissue was allowed to dissociate in Ca^{2+}- and Mg^{2+}-free Ringer solution for 30–60 min. The dissociated cells were plated onto glass coverslips and allowed to grow for 20–24 h (at 22–24 °C) prior to experimental use. Figure 1*A* and *B* illustrates typical motoneuron (n) and myocyte (m) morphology. The images were acquired with a cooled CCD camera (MCD-600, Spectra Source, Agoura Hills, CA, USA) on an inverted epifluorescence microscope (Diaphot, Nikon, Japan) using a ×40 objective lens (numerical aperture (NA), 0·75; Nikon). The

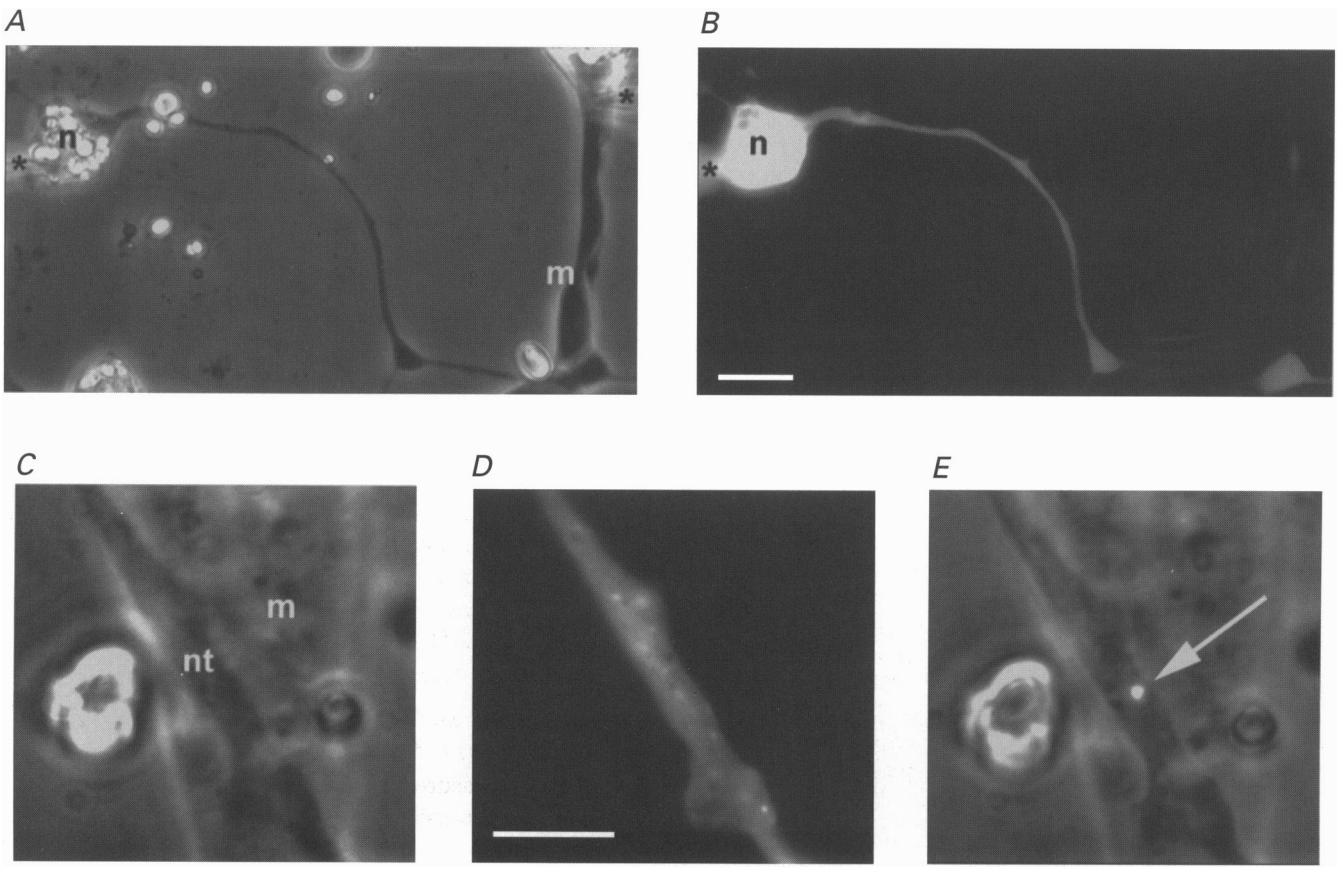

Figure 1. Morphology of cultured neuromuscular junctions: whole-cell patch clamp and fluorescence spot detection

A, phase-contrast image (×40 lens) of a cultured neuron (n) and myocyte (m) pair, which were simultaneously patch clamped (left and right; ∗). *B*, global epifluorescence image of the same neuron–myocyte pair. The neuronal patch pipette (left; ∗) contained 300 μM OGB-5N. Scale bar in *B* also applies to *A* and represents 20 μm. *C*, phase-contrast image of a nerve terminal (nt) contacting a myocyte (m) from a different cell pair using a ×100 objective lens. *D*, global fluorescence image of the same nerve terminal as in *C* (loaded with 300 μM OGB-5N). *E*, hybrid phase-contrast image with the fluorescence illumination spot (arrow) focused onto the nerve terminal. Scale bar in *D* also applies to *C* and *E* and represents 6 μm.

phase-contrast image in Fig. 1*A* shows a typical whole-cell patch configuration in which the neuronal patch electrode (left; *) was used to load the motoneuron with Ca^{2+} indicator, and the myocyte patch electrode (right; *) was used to assay evoked endplate synaptic currents (EPSCs). The Ca^{2+} indicator OGB-5N was allowed to diffuse throughout the cell body and axon for ~20 min subsequent to breakthrough and prior to optical recordings. In general, dialysis and diffusion times ranged from 10 to 60 min. Figure 1*B* shows a fluorescence image of the same cells in Fig. 1*A* obtained under global epi-illumination (100 W mercury lamp) using a standard dichroic cube (DM510, Nikon; excitation, 460–490 nm; emission, 520–560 nm).

Figure 1*C–E* documents the spot-detection system at a neuromuscular junction from which fluorescence transients were measured. The images were acquired using an oil-immersion objective lens (Plan Fluor Phase ×100, 1·3 NA; Nikon). Nerve terminals were visualized using either phase contrast (e.g. nt, Fig. 1*C*) or fluorescence (Fig. 1*D*) to identify a region of nerve–muscle contact where AP-induced fluorescence transients could be measured. The spot illumination/detection configuration was similar to that described previously (Escobar *et al.* 1994). A laser-illuminated pinhole (5 μm) was focused to a spot (arrow in Fig. 1*E*) through the ×100 objective lens on a selected nerve terminal. The full-width-half-maximal dimension of the illumination spot, measured with the CCD camera, was 0·7 μm. The illumination source was a multiline (457 nm, 488 nm, 514 nm) argon laser (5 W; model 168, Spectra Physics, Mountain View, CA, USA). Changes in Ca^{2+} indicator fluorescence were recorded by aligning and focusing the illumination spot on the photosensitive area (0·04 mm^2) of a photodiode (HR008; UDT, Hawthorne, CA, USA). Using the dimensions of the active area of the photodiode and the illumination spot, and according to confocal fluorescence theory (Wilson, 1990), the predicted detection volume was approximately $0·7 \times 0·7 \times 1·3\ \mu m^3$. The current output of the photodiode was amplified using an Axopatch-1B amplifier (50 GΩ feedback; Axon Instruments, Foster City, CA, USA). The output voltages were filtered with an 8-pole Bessel filter (Frequency Devices, Haverhill, MA, USA) at corner frequencies ranging from 300 Hz to 2 kHz.

Electrophysiology

Neuronal cell body APs and evoked EPSCs were recorded using a traditional whole-cell patch-clamp method (Yazejian *et al.* 1997). Cell body APs were recorded with an Axopatch 200B amplifier in 'I-fast' current-clamp mode and filtered at 5 kHz (4-pole Bessel). Na^+-dependent APs (Yazejian *et al.* 1997) were elicited by suprathreshold current pulses delivered to the neuronal cell body through the patch pipette. Myocytes were voltage clamped at a holding potential of −80 mV with an Axopatch-1A patch amplifier. AP-evoked EPSCs were filtered at 5 kHz.

Neuronal, myocyte, and fluorescence recordings were acquired at 14–56 kHz with a Digidata 1200A (Axon Instruments) data acquisition unit. The duration of the laser illumination required for acquiring fluorescence records was limited to between 400 to 500 ms to minimize local damage, usually indicated by increased baseline fluorescence and diminished signals. Consecutive records were obtained at intervals greater than 30 s to avoid accumulated damage. All experiments were performed at room temperature (19–21 °C).

Equilibrium properties of fluorescent Ca^{2+} indicators

In vitro calibrations of the Ca^{2+} indicators were performed using 10 μM of the indicator in Ca^{2+} standard solutions ranging from pCa 9 to 1 (Escobar, Velez, Kim, Cifuentes, Fill & Vergara, 1997). Aliquots of 5 μl were placed in the experimental chamber and their fluorescence was measured using the spot-detection system described above. The saturation curves demonstrated that both indicators exhibit a single Ca^{2+} binding site with a 1:1 stoichiometry. We determined the K_d of OGB-2 and OGB-5N to be 379 ± 49 nM and 32 ± 0·9 μM, respectively (±S.D., $n = 3$). Their maximum to minimum fluorescence ratio (F_{max}/F_{min}) was 29 ± 1·6 and 26 ± 0·7, respectively (±S.D., $n = 3$).

Data analysis

Consecutive fluorescence transients (2 to 8) detected from a single spot were averaged to improve the signal-to-noise ratio. A similar number of EPSCs were averaged to obtain a comparison with fluorescence transients. $\Delta F/F$ values were calculated using: $(F - F_{rest})/F_{rest}$, where F_{rest} is the mean resting fluorescence prior to stimulation and F is the time-dependent fluorescence. The decay phase of OGB-5N transients was fitted, using a least-squares fitting routine, to the following biexponential function.

$$F(t) = A_{fast}\exp(-t/\tau_{fast}) + A_{slow}\exp(-t/\tau_{slow}), \quad (1)$$

where t is time and A_{fast} and A_{slow} are the fitted amplitudes of the fast and slow components. The decay phases of OGB-2 fluorescence transients were fitted with a single exponential function (i.e. $A_{fast} = 0$).

The peak $\Delta F/F$ percentage change in experimental traces was used in combination with the K_d and F_{max}/F_{min} values of the indicators to estimate the free $[Ca^{2+}]$, assuming equilibrium conditions (Vergara & DiFranco, 1992).

RESULTS

Presynaptic Ca^{2+} transients elicited by single APs

Figure 2*A* shows an AP-elicited OGB-2 fluorescence transient (trace *b*) recorded at a nerve terminal using the spot-detection method. Trace *a* shows the AP recorded simultaneously at the neuronal cell body while the corresponding evoked EPSC is displayed in trace *c*. The fluorescence transient exhibited a rounded peak occurring well after the peak of the EPSC. The time at which one-half of the peak $\Delta F/F$ of this fluoresence transient was attained ($t_{½}$) was 2·8 ms. The decay phase of the fluorescence transient was fitted with a single exponential function (dotted line in trace *b*) with a time constant (τ_{slow}) of 59 ms.

Figure 2*B* shows the results from another cell loaded with the low affinity Ca^{2+} indicator OGB-5N. Unlike fluorescence transients measured using OGB-2, the AP-evoked OGB-5N fluorescence transient (trace *b*) had a time course that was more comparable to the corresponding EPSC (trace *c*). The rising phase of the fluorescence transient was much faster ($t_{½} = 0·4$ ms) and the peak was sharper than that of the OGB-2 fluorescence transient (Fig. 2*A*). Moreover, the decay of the transient displayed an initial rapid phase, followed by a slower decay towards baseline. We fitted this decay portion of the fluorescence transient with a biexponential function (eqn (1)), yielding a τ_{fast} of 1·7 ms and a τ_{slow} of 62 ms. The magnitude of the contribution of the slow component was smaller than that of the fast component ($A_{slow} = 0·4A_{fast}$).

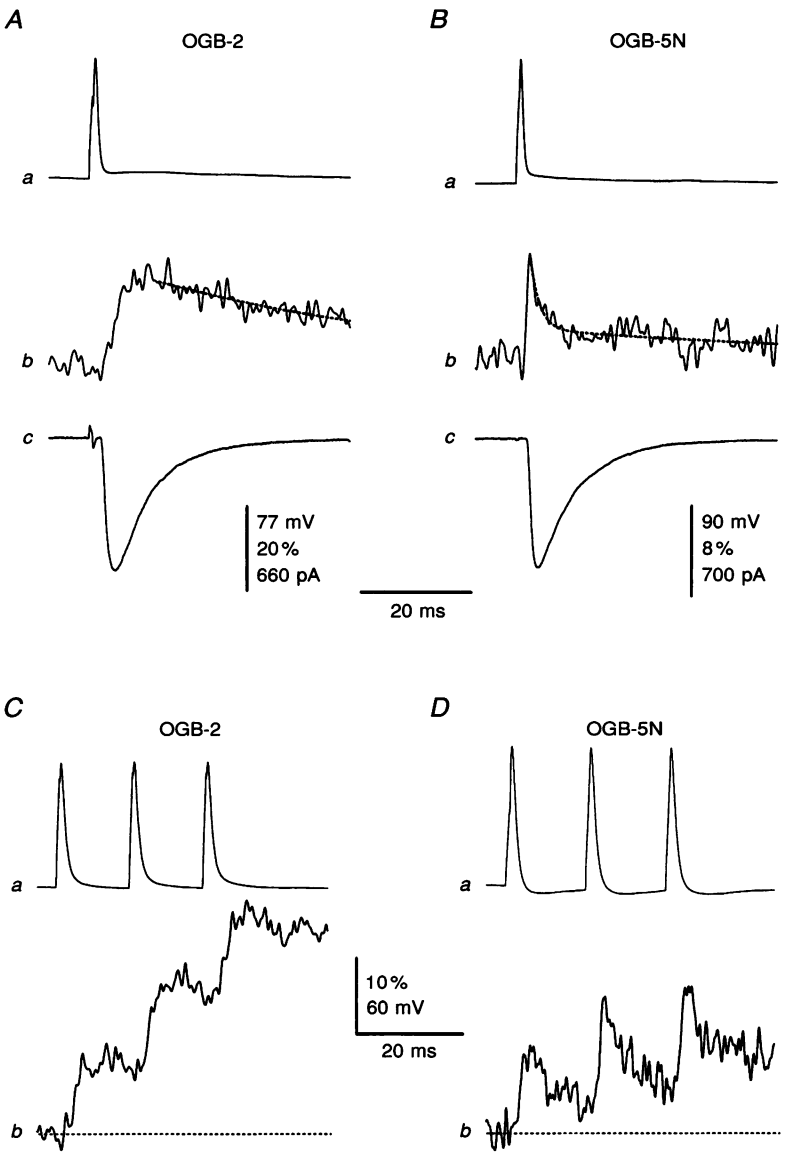

Figure 2. Presynaptic Ca^{2+} transients and EPSCs elicited by neuronal action potentials

A, neuronal AP, nerve terminal fluorescence transient using 50 μM OGB-2, and associated EPSC. *a*, AP record recorded under current-clamp conditions (resting potential, 66 mV). *b*, OGB-2 fluorescence transient obtained using the spot-detection method. The dotted line is a single exponential function fitted to the decay phase of the fluorescence transient ($\tau_{slow} = 59$ ms). *c*, AP-elicited EPSC monitored under voltage-clamp conditions. The small bipolar inflection in the EPSC record resulted from a voltage pulse delivered to the cell body to monitor the series resistance. All traces were acquired simultaneously and represent an average of three records. The fluorescence signal was filtered at 1 kHz, acquired at 56 kHz, smoothed off-line using a 2·7 kHz FFT (fast Fourier transform) digital filter and presented as a $\Delta F/F$ percentage. *B*, an experiment identical to that in *A*, except that 300 μM OGB-5N was used in the neuronal pipette solution. *a*, neuronal AP (resting potential, 72 mV). *b*, OGB-5N fluorescence. The dotted line is a fitted biexponential decay function (eqn (1), Methods) yielding a τ_{fast} of 1·7 ms with A_{fast}, 0·067 and a τ_{slow} of 62 ms with A_{slow}, 0·027. *c*, EPSC measured earlier in the experiment using an identical action potential to that shown in *a*. Traces represent averages of five consecutive sweeps. They were acquired and processed identically to those shown in *A*. *Ca*, three APs, separated by 15 ms, elicited in the neuronal cell body. The neuronal patch pipette contained 50 μM OGB-2. Resting potential, 64 mV. *b*, OGB-2 fluorescence transients detected in response to APs shown in *a*. The fluorescence record was filtered at 500 Hz and acquired at 14 kHz. *Da*, train of APs elicited in a different motoneuron. The neuronal patch pipette contained 300 μM OGB-5N. Resting potential, 62 mV. *b*, elicited OGB-5N fluorescence transients. Records were filtered at 1 kHz, acquired at 56 kHz, and smoothed using a 2·7 kHz digital FFT filter. Dotted lines in *C* and *D* indicate the mean baseline fluorescence. Fluorescence records in *C* and *D* were presented as a $\Delta F/F$ percentage. Data in *C* and *D* are averages of three traces.

Table 1. Summary of OGB-2 and OGB-5N fluorescence transient characteristics

	Peak $\Delta F/F$ (%)	$t_{½}$ (ms)	τ_{fast} (ms)	τ_{slow} (ms)	A_{slow}/A_{fast}
OGB2	14 ± 7 (15)*	1·8 ± 0·6 (14)*	—	73 ± 34 (12)†	—
OGB-5N	8·5 ± 2·9 (13)	0·54 ± 0·27 (13)	1·9 ± 0·6 (11)	50 ± 24 (11)	0·5 ± 0·26 (11)

Data are presented as means ± S.D., n values are shown in parentheses. Peak $\Delta F/F$ is the averaged maximum $\Delta F/F$ attained at a single spot location; τ_{fast}, τ_{slow}, A_{fast} and A_{slow} are parameters of eqn (1) (see Methods). * $P < 0·001$, † $P > 0·5$, compared with OGB-5N; Student's t test.

Table 1 summarizes the fluorescence transient data from several nerve terminals using OGB-2 and OGB-5N. The rate of rise of the OGB-5N fluorescence transients was significantly faster than that of the OGB-2 transients. Moreover, the fast decay component of the OGB-5N transients was not observed in the OGB-2 transients. Nevertheless, the mean τ_{slow} values of OGB-5N and OGB-2 transients were not significantly different ($P > 0·5$).

Sensitivity of presynaptic Ca^{2+} transients to Cd^{2+}

To demonstrate that fluorescence transients were dependent on presynaptic Ca^{2+} entry through voltage-gated Ca^{2+} channels during the AP (Yazejian *et al.* 1997), we added 100 μM Cd^{2+} to the external solution. We found that the OGB-5N fluorescence transients were completely blocked ($n = 3$; data not shown). When rinsed with NFR in the absence of Cd^{2+}, the block was reversed.

Presynaptic Ca^{2+} transients elicited by a brief train of APs

To further explore the presynaptic Ca^{2+} dynamics depicted by high and low affinity indicators, we investigated their response to tetanic stimulation. Figure 2*C* shows an OGB-2 fluorescence signal (trace *b*) elicited by a train of three APs at 15 ms intervals (trace *a*). Figure 2*D* illustrates the results from a different cell in which a similar train (trace *a*) elicited an OGB-5N fluorescence record (trace *b*). Although every AP (within each train) produced approximately equal fluorescence increases, the pattern of $[Ca^{2+}]$ change reported by each indicator was different. The OGB-2 fluorescence trace displayed 'staircase' fluorescence increases that, after the third AP, reached a level nearly 3-fold higher than that obtained after a single response. In contrast, the OGB-5N record exhibited a pattern in which each AP elicited similar transients with individual decay phases that did not fully return to baseline (Fig. 2*B*). Hence, at this frequency of stimulation, there was a relatively small build-up of fluorescence by the end of the train.

Presynaptic Ca^{2+} transients precede neurotransmitter release

Previous studies using this preparation have documented the temporal relationship between the presynaptic Ca^{2+} current during an AP and the evoked EPSC (Yazejian *et al.* 1997). The delay between the maximum rate of rise of the Ca^{2+} current and the onset of the EPSC was approximately 700 μs. To investigate the kinetic relationship between the $[Ca^{2+}]$ increase and neurotransmitter release, we recorded OGB-5N transients simultaneously with corresponding EPSCs. Figure 3*A* shows the results of one experiment on an expanded time scale; for clarity we inverted the EPSC and plotted it as a thin continuous line. The rising phase of the OGB-5N transient clearly precedes that of the EPSC. The delay between the onset of the Ca^{2+} transient and that of the EPSC was approximately 800 μs, comparable to the delay observed for the Ca^{2+} current (Yazejian *et al.* 1997). Interestingly, in five out of six nerve terminals stained with OGB-5N, a significant fluorescence increase was observed prior to neurotransmitter release, whereas OGB-2 transients did not (from 4 nerve terminals) exhibit a detectable fluorescence increase preceding the onset of the EPSC.

DISCUSSION

We show that AP-induced presynaptic fluorescence transients, obtained using a low affinity Ca^{2+} indicator, the spot-detection method, and patch-clamp techniques, exhibit the fast kinetic properties expected to underlie excitation–release coupling at a neuromuscular junction.

An important feature of the cultured neuromuscular junction is that the cell body of isolated motoneurons could be whole-cell patch clamped, thus permitting the dialysis of nerve terminals with membrane-impermeant Ca^{2+} indicators. This minimized fluorescence contamination from other cells (e.g. postsynaptic myocyte) and enabled us to assay Ca^{2+} dynamics in small, localized regions (0·7 × 0·7 × 1·3 μm) of the terminal using fluorescence spot detection. Interestingly, only a few spot-detection sites at the presynaptic terminal yielded Ca^{2+} transients. Figure 3*B* illustrates dramatic differences in the Ca^{2+} transients detected at two consecutive locations of the same nerve terminal. These data are consistent with the presence of $[Ca^{2+}]$ domains along the area of contact between indicator-loaded nerve terminals and myocytes.

The blockage of AP-induced fluorescence transients by Cd^{2+} is consistent with their dependence on extracellular Ca^{2+}

entry, presumably via N-type voltage-gated channels, which have been shown to generate the Ca^{2+} current underlying neurotransmitter release in this preparation (Yazejian *et al.* 1997). We have also found that 100 μM Cd^{2+} blocks isolated inward Ca^{2+} currents in voltage-clamped nerve terminals (D. A. DiGregorio & J. L. Vergara, unpublished observations). Furthermore, OGB-5N fluorescence transients (Figs 2*B* and 3*A*) attained peak fluorescence with a time course ($t_{½}$ = 0·54 ms) compatible with the brief duration of Ca^{2+} entry during an AP (Yazejian *et al.* 1997).

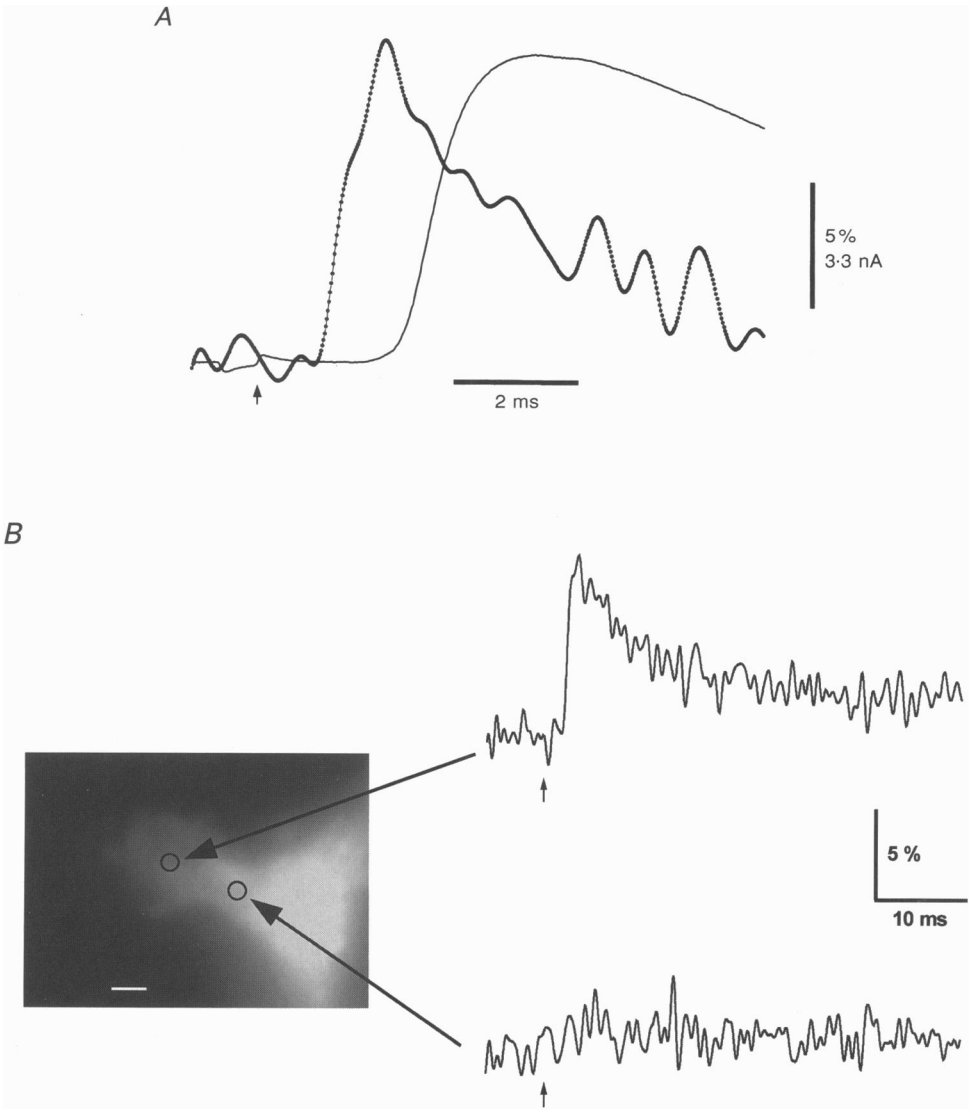

Figure 3. OGB-5N fluorescence transients measured simultaneously with an EPSC and detected at different locations in a nerve terminal

A, OGB-5N fluorescence transient (thick trace) elicited in response to a single AP (not shown) superimposed with an inverted trace of the EPSC. The fluorescence trace represents an average of four consecutive records. The EPSC is an average of three of the four corresponding current records. The fluorescence data were filtered at 2 kHz, acquired at 56 kHz, smoothed using a 2·7 kHz digital FFT filter and scaled as a $\Delta F/F$ percentage. *B*, fluorescence CCD image (left) of a dye-loaded nerve terminal acquired following the detection of AP-induced OGB-5N fluorescence transients (right traces). The large arrows point to the location at which each fluorescence transient was recorded. The open circles approximately delineate the regions of illumination and detection. Both fluorescence traces correspond to an average of three consecutive recordings and were filtered at 2 kHz, acquired at 56 kHz, smoothed using a 1·8 kHz digital FFT filter, and scaled as a $\Delta F/F$ percentage. The upper trace was obtained subsequent to the lower trace. The scale bar represents 1 μm. In *A* and *B*, the small arrows indicate the end of the current stimulus.

The records in Fig. 2 and the data summarized in Table 1 illustrate that the kinetics of OGB-2 fluorescence transients are slower than that of OGB-5N transients. These results can be explained given that low affinity indicators are less liable to depict a distorted time course of underlying fast $[Ca^{2+}]$ changes than are higher affinity indicators (Escobar *et al.* 1994; Regehr & Atluri, 1995; Escobar *et al.* 1997). If it is assumed that OGB-5N and OGB-2 have the same association rate constant, the former would track a $[Ca^{2+}]$ change with ~100-fold better response time (Escobar *et al.* 1997). Thus, our OGB-5N transients depict a rapid transient $[Ca^{2+}]$ change with a $t_{½}$ of 0·54 ms. This result is slightly faster than those obtained in multicellular preparations using furaptra (Sabatini & Regehr, 1996; Sinha *et al.* 1997).

Most preparations in which AP-induced presynaptic Ca^{2+} transients have been measured using low affinity indicators do not exhibit the rapid decay phase (τ, ~2 ms) present in our OGB-5N transients (however, see Sugimori, Lang, Silver & Llinás, 1994). In multicellular preparations the $t_{½}$ of decay ranged between 30 and 40 ms (Regehr & Atluri, 1995; Sinha *et al.* 1997), and in the synapse of Held, the decay time constant was found to be 100 ms (Helmchen, Borst & Sakmann, 1997). We believe that the rapid increase and rapid decay of OGB-5N transients result from two putative features of AP-induced presynaptic $[Ca^{2+}]$ changes (Llinás *et al.* 1995): (1) a rapid Ca^{2+} entry, and (2) a rapid dissipation of a $[Ca^{2+}]$ gradient by diffusion. We calculate, assuming indicator equilibration, that the mean peak $\Delta F/F$ of the OGB-5N transient (8·5%) corresponds to a $[Ca^{2+}]$ change of ~120 nM. This value is orders of magnitude lower than the 100–500 μM estimated to occur in close proximity to presynaptic Ca^{2+} entry sites (Fogelson & Zucker, 1985; Simon & Llinás, 1985; Roberts, 1994). However, our experimental data can be reconciled with theoretical predictions of the high $[Ca^{2+}]$ within such microdomains if we consider that our spot-detection volume (0·6 μm^3) may contain a few microdomains with each increasing the $[Ca^{2+}]$ to, for example, 100 μM. If we assume that OGB-5N transients result predominantly from indicator molecules binding Ca^{2+} within the volume of a microdomain, and that that volume is $\sim 5 \times 10^{-4}$ μm^3 (Roberts, 1994), then a single microdomain would produce a $\Delta F/F$ increase of ~6%. In essence, OGB-5N fluorescence transients were scaled by the resting fluorescence of the much larger spot volume. In the case of OGB-2 fluorescence transients, indicator saturation and poor kinetic characteristics may contribute to the even lower estimate of the peak $[Ca^{2+}]$ change (22 nM for a $\Delta F/F$ of 14%, assuming 100 nM resting). Hence, the kinetic profile of OGB-5N fluorescence transients may approximate the $[Ca^{2+}]$ change 'seen' by the Ca^{2+} sensor responsible for the release of neurotransmitter at the active zone.

Augustine, G. J., Charlton, M. P. & Smith, S. J. (1987). Calcium action in synaptic transmitter release. *Annual Review of Neuroscience* **10**, 633–693.

Charlton, M. P., Smith, S. J. & Zucker, R. S. (1982). Role of presynaptic calcium ions and channels in synaptic facilitation and depression at the squid giant synapse. *Journal of Physiology* **323**, 173–193.

Escobar, A. L., Monck, J. R., Fernandez, J. M. & Vergara, J. L. (1994). Localization of the site of Ca^{2+} release at the level of a single sarcomere in skeletal muscle fibres. *Nature* **367**, 739–741.

Escobar, A. L., Velez, P., Kim, A. M., Cifuentes, F., Fill, M. & Vergara, J. L. (1997). Kinetic properties of DM-nitrophen and calcium indicators: rapid transient response to flash photolysis. *Pflügers Archiv* **434**, 615–631.

Fogelson, A. L. & Zucker, R. S. (1985). Presynaptic calcium diffusion from various arrays of single channels. Implications for transmitter release and synaptic facilitation. *Biophysical Journal* **48**, 1003–1017.

Helmchen, F., Borst, J. G. & Sakmann, B. (1997). Calcium dynamics associated with a single action potential in a CNS presynaptic terminal. *Biophysical Journal* **72**, 1458–1471.

Katz, B. (1969). *The Release of Neural Transmitter Substances.* Liverpool University Press, Liverpool.

Llinás, R. & Nicholson, C. (1975). Calcium role in depolarization–secretion coupling: an aequorin study in squid giant synapse. *Proceedings of the National Academy of Sciences of the USA* **72**, 187–190.

Llinás, R., Sugimori, M. & Silver, R. B. (1995). The concept of calcium concentration microdomains in synaptic transmission. *Neuropharmacology* **34**, 1443–1451.

Miledi, R. & Parker, I. (1981). Calcium transients recorded with arsenazo III in the presynaptic terminal of the squid giant synapse. *Proceedings of the Royal Society* B **212**, 197–211.

Regehr, W. G. & Atluri, P. P. (1995). Calcium transients in cerebellar granule cell presynaptic terminals. *Biophysical Journal* **68**, 2156–2170.

Roberts, W. M. (1994). Localization of calcium signals by a mobile calcium buffer in frog saccular hair cells. *Journal of Neuroscience* **14**, 3246–3262.

Sabatini, B. L. & Regehr, W. G. (1996). Timing of neurotransmission at fast synapses in the mammalian brain. *Nature* **384**, 170–172.

Simon, S. M. & Llinás, R. R. (1985). Compartmentalization of the submembrane calcium activity during calcium influx and its significance in transmitter release. *Biophysical Journal* **48**, 485–498.

Sinha, S. R., Wu, L. G. & Saggau, P. (1997). Presynaptic calcium dynamics and transmitter release evoked by single action potentials at mammalian central synapses. *Biophysical Journal* **72**, 637–651.

Sugimori, M., Lang, E. J., Silver, R. B. & Llinás, R. (1994). High resolution measurement of the time course of calcium-concentration microdomains at squid presynaptic terminals. *Biological Bulletin* **187**, 300–303.

Vergara, J. & DiFranco, M. (1992). Imaging of calcium transients during excitation–contraction coupling in skeletal muscle fibers. *Advances in Experimental Medicine and Biology* **311**, 227–236.

Wilson, T. (1990). *Confocal Microscopy.* Academic Press, New York.

YAZEJIAN, B., DIGREGORIO, D. A., VERGARA, J. L., POAGE, R. E., MERINEY, S. D. & GRINNELL, A. D. (1997). Direct measurements of presynaptic calcium and calcium-activated potassium currents regulating neurotransmitter release at cultured *Xenopus* nerve–muscle synapses. *Journal of Neuroscience* **17**, 2990–3001.

ZUCKER, R. S. & FOGELSON, A. L. (1986). Relationship between transmitter release and presynaptic calcium influx when calcium enters through discrete channels. *Proceedings of the National Academy of Sciences of the USA* **83**, 3032–3036.

Acknowledgements

This work was supported by a grant from the National Institutes of Health (AR25201 to J.L.V.) and by MSTP (GM 08042) and Individual (NS10197) Fellowships from National Institutes of Health to D.A.D. We thank Hyun-Wook Lee and Lee Chen for preparation of the cell cultures. We would also like to thank Jeremy Dittman, Alan Grinnell, Susan Kerr, Albert Kim and Jonathan Monck for helpful comments on the manuscript.

Author's email address

J. L. Vergara: jvergara@physiology.medsch.ucla.edu

Received 27 August 1997; accepted 16 October 1997.